PHARMACIA

Pharmacia 71: 1–15
DOI 10.3897/pharmacia.71.e138556

Research Article

Unveiling the anticancer potential of the ethanolic extract from *Pometia pinnata*: Molecular dynamics targeting CHK1 and cytotoxicity study on MCF-7 cells

Henny Sri Wahyuni[1], Marianne[2], Sony Eka Nugraha[3], Imam Bagus Sumantri[3], Clara Claudia Jap[1], Thomi Baihaki Hijriyan[1]

1 *Department of Pharmaceutical Chemistry, Faculty of Pharmacy, Universitas Sumatera Utara, Medan 20155, Indonesia*
2 *Department of Pharmacology, Faculty of Pharmacy, Universitas Sumatera Utara, Medan 20155, Indonesia*
3 *Department of Pharmaceutical Biology, Faculty of Pharmacy, Universitas Sumatera Utara, Medan 20155, Indonesia*

Corresponding author: Henny Sri Wahyuni (henny@usu.ac.id)

Received 4 October 2024 ♦ **Accepted** 12 November 2024 ♦ **Published** 9 December 2024

Citation: Wahyuni HS, Marianne, Nugraha SE, Sumantri IB, Jap CC, Hijriyan TB (2024) Unveiling the anticancer potential of the ethanolic extract from *Pometia pinnata*: Molecular dynamics targeting CHK1 and cytotoxicity study on MCF-7 cells. Pharmacia 71: 1–15. https://doi.org/10.3897/pharmacia.71.e138556

Abstract

Cancer remains one of the most lethal diseases globally, with CHK1 being a critical pathway frequently altered in cancer progression. This study evaluated the anticancer and cytotoxic properties of the ethanol extract of Matoa (*Pometia pinnata*) leaves in silico and in vitro. Maceration was conducted to obtain the ethanol extract with physicochemical, pharmacokinetic, and toxicity predictions conducted using Lipinski's Rule of Five, pkCSM, and Pro-Tox II. Molecular docking was performed using Autodock Vina and DOCK6.2, followed by molecular dynamic simulations using GROMACS. Cytotoxicity assays on MCF-7 cells were carried out using the MTT methods. The results demonstrated that the extract tested positive for flavonoids, alkaloids, tannins, saponins, glycosides, and steroids. The extract also shows potential inhibitory activity against CHK1, supported by favorable binding affinities and critical amino acid interactions. Additionally, the extract exhibited a moderate cytotoxic effect on cell MCF-7 with an IC_{50} of 139 µg/mL.

Keywords

IC50, in silico, in vitro, MCF-7, *Pometia pinnata*

Introduction

Cancer remains one of the most significant public health challenges globally, with its prevalence and mortality rates continuing to rise. According to the global cancer observatory (GCO) 2020 data, an estimated 19.3 million new cancer cases and nearly 10 million cancer deaths occurred worldwide in 2020. A multicenter study conducted by the Indonesian Radiation Oncology Society (IROS) highlighted that breast cancer, followed by cervical, nasopharyngeal, lung, and rectal cancers, are the most common types of cancer in Indonesia (GCO 2020; Jayalie et al. 2023). This staggering figure underscores the fact that cancer

recurrence is more common compared to other diseases and is challenging to treat due to delayed diagnosis and the development of resistance to chemotherapy.

Cancer is initiated by the accumulation of genetic alterations and genomic insults through exogenous (UV and chemical radiation) and endogenous factors (free radicals and alkylating agents during metabolic processes). This led to cell damage and caused up to 10^5 lesions/cell/day. DNA lesions then affect crucial processes such as DNA transcription and replication and even cause double-strand breaks. As a response to these damages, cells are equipped with DNA damage response that plays a significant role in maintaining genomic stability and the integrity of DNA. DDR is triggered by a signal of damaged DNA, activating the cell cycle checkpoints, DNA repair mechanism, DNA damage adaptation, and cell death. Two central serine/threonine kinases regulate these processes, CHK1 (Shin and Cho 2023).

As a response to single-strand DNA breaks, the ATR-CHK1 signaling pathway will be activated by single-strand DNA breaks. Activation of CHK1 initiates the arrest of cell cycle progression in phase G2/M, which allows the DNA to be repaired or possibly cell death. CHK1 caused cell cycle arrest in phase G2/M by phosphorylating the CDC25C (cell division cycle 25C), which prevents the activation of CDK1 (cyclin-dependent kinase 1), providing time to resolve the DNA damage (Manic et al. 2015; Ronco et al. 2016).

In human neoplasms, CHK1 is frequently upregulated and overexpressed, especially in triple-negative breast cancer carcinomas (TNBC) and MYC-neuroblastoma-related (MYCN)-amplified and high-risk tumors. Based on this, it can be concluded that overexpression, mutation, and the loss of CHK1 are responsible for most cancer cases. Therefore, targeting CHK1 in cancer cells has become crucial to halting cancer progression (Manic et al. 2015).

The importance of inhibiting CHK1 has led to the development of their inhibitors. Prexasertib is a selective ATP inhibitor of CHK1 that causes DNA DSBs in the S-phase cell cycle and removes the protection of the DNA checkpoint. Prexasertib was also reported to induce the accumulation of unrepaired cells in the S-phase, reflecting the accumulation of DNA damage in the cell, leading to cell death or apoptosis. Prexasertib has completed a phase II clinical trial for its use as a single anticancer agent or in combination with other anti-neoplastic drugs. Despite its activity as a selective inhibitor of CHK1, its efficacy still needs to be monitored because, in some cases, Prexasertib has been reported to cause serious adverse effects. This underscores the importance of finding compounds that can act as multi-target inhibitors of CHK1 with minimal side effects (Ronco et al. 2016; Nikolaev and Yang 2020).

Matoa (*Pometia pinnata*) is a traditional Asian medicine that treats fever and skin infections. This plant's wood and bark extracts have demonstrated antioxidant properties, while the leaf extracts exhibit antifungal activity against *Phytophthora infestans* and also show potent inhibitory activity against HIV-1 integrase (IN). Previous studies have identified flavonoids as the major bioactive compounds in these extracts. Flavonoids are known for their diverse biological activities, including anti-inflammatory, antiallergic, antiviral, and antioxidant effects. Additionally, phenolic compounds have been reported to possess astringent, antibacterial, and antidiarrheal properties (Razoki 2023). Kaempferol-3-O-rhamnoside and quercetin-3-O-rhamnoside are two flavonoids isolated from *Pometia pinnata* leaf ethanol extract, which has shown antioxidant and antibacterial effects against *Bacillus subtilis*, *Staphylococcus aureus*, and *Escherichia coli* (Wiart 2006; Suedee et al. 2013). However, research on the anticancer potential of *Pometia pinnata* is limited. This study aims to explore the anticancer activity of *Pometia pinnata* using both in silico and in vitro approaches.

In silico methods are commonly used to screen potential compounds in drug discovery. Molecular docking predicts the interaction between the protein-ligand complexes in 3D geometry. In order to predict the protein-ligand complexes further to their molecular system, molecular dynamics need to be employed. Molecular dynamic simulations can capture crucial biomolecular processes, such as ligand binding, protein folding, and conformational changes, and even predict how biomolecules respond at an atomic level to signaling, such as protonation, phosphorylation, or mutation. Prediction of a potential compound's physicochemical, pharmacokinetic, and toxicity properties was also part of in silico computational methods, where it plays a big part in forecasting the properties of the potential compound as a drug candidate, minimizing the need for animal research. It can also screen chemical compounds for further testing based on their ADMET qualities to reach the desired compound and obtain possible effectiveness against the targeted illness. Based on that, in silico has become a more accessible and powerful method by providing a vast amount of data and implementing a considerable budget reduction needed for the development of new drug candidates (de Ruyck et al. 2016; Hollingsworth and Dror 2018; Navien et al. 2021; Yusuf 2023).

Following the initial screening of potential candidates using in silico methods, in vitro testing is pivotal in validating the compound's efficacy. In vitro assays provide a controlled environment where the behavior of cancer cells can be closely monitored under various conditions. MCF-7 is a breast cancer cell line that is estrogen receptor (ER)-positive, progesterone receptor (PR)-positive, and HER2-negative. This cell is commonly used in developing chemotherapeutic drugs due to its sensitivity to various cancer agents. One of the most common methods used to assess the cytotoxic effects of compounds on MCF-7 cells is the MTT assay. The MTT assay measures the reduction of 3-(4,5-dimethylthiazol-2-yl)-2,5-diphenyltetrazolium bromide (MTT) to formazan, which is directly proportional to the number of viable cells. This method allows for determining the IC50 value, representing the compound concentration required to inhibit cell growth by 50%. The results from these assays help in identifying compounds that exhibit significant cytotoxicity against MCF-7 cells,

thereby indicating their potential as anticancer agents (Edirweera et al. 2018; Kitaeva et al. 2020; Purwaningsih et al. 2021). Therefore, this study is conducted to obtain the activity of compounds contained in the ethanol extract of *Pometia pinnata* leaves through in silico and in vitro assays to determine their ability as anticancer agents in MCF-7 cells.

Materials and methods

Materials

The materials used include a hardware device, a computer with 11th Gen Intel® Core™ i9-11900KF, RTX 2060 16 GB NVME 3.50 GHz, RAM 64 GB DDR 4, SSD 1,8 T, software DOCK6.2, Avogadro, CHARMM-GUI website (https://www.charmm-gui.org/), Discovery Studio (Systemes 2016), Lipinski's Rule of Five website (https://www.scfbio-iitd.res.in/software/drugdesign/lipinski.jsp), Grace, GMX Tools, GROMACS 2022.4 (Bauer et al. 2022), pkCSM Online Tools website (https://biosig.lab.uq.edu.au/pkcsm/), proTOX-II website (https://tox.charite.de/protox3/), Protein Data Bank website (https://rcsb.org/), and PubChem website (https://pubchem.ncbi.nlm.nih.gov/).

Ethical approval

This study has obtained ethical approval No. 0670/KEPH-FMIPA/2021 from the Animal Research Ethics Committee of the Faculty of Mathematics and Natural Sciences, Universitas Sumatera Utara.

Methods

Extraction and phytochemical screening of Pometia pinnata *leaves*

The extraction process was conducted through maceration using 96% ethanol added at a sample-to-solvent ratio of 1:2 (w/v). The mixture was then filtered through a Buchner funnel with a vacuum pump to separate the extract from the residue. The solvent was subsequently removed from the extract using a rotary evaporator to produce a concentrated form. Phytochemical screening was conducted for specific compounds: flavonoids were detected using magnesium powder, alkaloids with Dragendorff's reagent, tannins with $FeCl_3$, glycosides with Molisch's reagent, saponins by observing foam formation, and steroids with the Liebermann-Burchard reagent (Praptiwi et al. 2020; Razoki 2023).

Prediction of physicochemical, pharmacokinetics, and toxicity of ethanol extract of Pometia pinnata *leaves*

The 3D structure of 20 compounds contained in ethanol extract of *Pometia pinnata* leaves, which are: Apigenin 7-O-diglucuronide, benzene, pigallocatechin, gallic acid, jasmonic acid, kaempferol, kampferol-3-O-glucoside (astragalin), kaempferol-3-O-rhamnoside (afzelin), nicotiflorin, p-coumaroyl glycolic acid, phenol, p-hydroxybenzaldehyde, quercetin, quercetin-3-Oglucoside (isoquercetin), quercetin-3-O-rhamnoside (quercitrin), quercetin-3-O-glucosyl-(1→4)-rhamnoside (rutin), syringic acid, tannin, vanillic acid, vanillin were downloaded from PubChem in *pdb and *smi format and was subjected to physicochemical prediction by Lipinski's Rule of Five by submitting the compounds in the website and the pH was set in 7. The results are then saved. The smiles were submitted for the pharmacokinetics and toxicity prediction, and the prediction was run; the results were then saved.

Protein and ligand preparation

Protein and ligand preparation was conducted twice for each software used. For AutoDock Vina docking, AutoDock Tools was utilized to prepare the proteins and ligands by separating CHK1 from the native ligands, YEX, and removing water molecules. Polar hydrogens were added, computed Gasteiger charges were calculated, and a grid box of 40 × 40 × 40 Å was set to cover the protein's active site. The ligand and receptor were converted into PDBQT format. In the case of DOCK6.2, the protein and native ligands were separated using GNINA via the terminal. Hydrogen atoms were added, GAFF force fields were applied, and the geometry was optimized using Avogadro (Trott and Olson 2010; McNutt et al. 2021).

Molecular docking of ethanol extract compounds against CHK1

The docking process started by doing docking validation of the receptors and the native ligand using Autodock Vina by setting the exhaustiveness to 32. The RMSD was calculated using Pymol. For the docking process by Autodock Vina, the grid box of the ligand and receptor was constructed, and the exhaustiveness was set to 32, then run. The binding affinity results are then saved in Excel. The docking process through DOCK6.2 required building the ligands' sphere; before the docking process started, energy minimization was carried out first and followed by rigid and flexible docking. The grid score results are saved in Excel. Visualization of the docking results was carried out using Biovia Discovery Studio Client 2021 by inserting the clean receptor file and the output ligands file, resulting in the interaction of ligands and the receptor in the form of amino acid residues (Trott and Olson 2010; McNutt et al. 2021).

Molecular dynamic simulations of ethanol extract compounds against CHK1

From the docking results, five chosen compounds were subjected to further testing with MD simulations. The ligand-receptor complexes were built using the output file from the docking. The complex file was then submitted through CHARMM-GUI to obtain the output file for MD simulations. The ionization throughout the simulations was changed to NaCl with GROMACS as the force field. A 250 ps NVT (constant number of particles, volume, and

temperature) ensemble was used for equilibration, and a 250 ps NPT (constant number of particles, pressure, and temperature) ensemble was selected for dynamics input generation. The temperature was set to 310°K, and the input file was generated and extracted from the .tgz file. A molecular dynamics simulation was conducted using GROMACS 2022.4, which involved 5000 steps of energy minimization and a 50 ns simulation with a four fs-time step. The binding energy calculations were based on 200 snapshots extracted from the last 10 ns of the 100 ns simulation. Grace was used to visualize the ligands' RMSD, RMSF, SASA, and hydrogen bonds. Additionally, MMPBSA calculations were conducted using the g-mmpbsa tool (Lee et al. 2016; Bauer et al. 2022).

Cell culture

MCF-7, a human breast adenocarcinoma cell line, was provided from the cell culture collection of the Laboratory of Parasitology, Faculty of Medicine, Public Health, and Nursing, Universitas Gadjah Mada, Indonesia. MCF-7 cells were cultivated in Dulbecco's Modified Eagle Medium (DMEM) supplemented with 10% fetal bovine serum (FBS), 2% penicillin-streptomycin, and 0.5% amphotericin B (CCRC 2009).

Cytotoxicity assay of ethanol extract of Pometia pinnata *leaves to MCF-7 cells*

The cytotoxicity assay begins by preparing the DMEM media by mixing one sachet of DMEM with 2 g of HEPES and 2 g of $NaHCO_3$ in an Erlenmeyer flask containing 800 ml of sterile water. The pH is adjusted to 7.2–7.4 by adding 1N HCl or NaOH. The solution is then topped up to 1 liter with sterile water, sterilized using a vacuum filter, and aliquoted into 500 ml bottles for storage at 2–8 °C. In a laminar flow cabinet, the media is supplemented with 10% fetal bovine serum (FBS), 2% penicillin-streptomycin, and 0.5% amphotericin B and stored at 2–8°C. Cells from frozen storage are thawed, mixed with 10 ml of media, and centrifuged at 600 rpm for 5 minutes. The supernatant is discarded, and the cells are resuspended in 4 ml of culture media. The suspension is divided between new culture flasks with 5 ml of media and incubated in a CO_2 incubator. Cells are observed under an inverted microscope daily. The MCF-7 cells are harvested, washed twice with PBS, treated with 0.25% trypsin-EDTA, incubated for 3–5 minutes, and then neutralized with 4 ml of media. The cells are resuspended and counted using a hemocytometer. For testing, 5 mg of the test compound is dissolved in 100 µl of DMSO and diluted to the required concentrations. A concentration series is prepared with a concentration of 1000 µg/mL, 500 µg/mL, 250 µg/mL, 125 µg/mL, and 62.5 µg/mL for ethanol extract of *Pometia pinnata* leaves and 50 µg/mL, 25 µg/mL, 12.5 µg/mL, 6.125 µg/mL, and 3.125 µg/mL for doxorubicin as a positive control. MCF-7 cells (1×10^4 cells/100 µl) are distributed into a 96-well plate and incubated for 24 hours before treatment with the prepared compounds (CCRC 2009).

Results and discussion

Phytochemical screening of ethanol extract of *Pometia pinnata*

The phytochemical screening of the ethanol extract of *Pometia pinnata* leaves was done to identify several bioactive compounds. The results can be seen in Table 1.

Table 1. Bioactive compounds of ethanol extract of *Pometia pinnata* leaves.

Bioactive compounds	Results
Flavonoids	Positive
Alkaloids	Positive
Tannins	Positive
Saponins	Positive
Glycosides	Positive
Steroids	Positive

From the table above, it can be seen that the ethanol extract of *Pometia pinnata* leaves tested positive for flavonoids, alkaloids, tannins, glycosides, saponins, and steroids, which are associated with potential anticancer activity. Flavonoids are known for their antioxidant properties, which help protect cells from oxidative stress and can induce apoptosis in cancer cells. Alkaloids exhibit cytotoxic effects by interfering with DNA replication and protein synthesis, leading to cell cycle arrest, while tannins possess anti-inflammatory and antioxidant activities that can inhibit tumor growth by modulating key signaling pathways. Saponins can induce apoptosis and disrupt cancer cell membranes, while glycosides enhance the solubility and bioavailability of other active compounds, supporting their therapeutic potential. Lastly, steroids may influence growth-related signaling pathways and enhance the efficacy of chemotherapeutic agents. The presence of these compounds in *Pometia pinnata* leaves suggests a synergistic effect that could enhance their overall anticancer activity (Rajasekar et al. 2021; Dhyani et al. 2022; Duyen et al. 2022; Roy et al. 2022).

Analysis of physicochemical, pharmacokinetic, and toxicity properties

The physicochemical prediction includes molecular weight, logP, hydrogen bond donor, and hydrogen bond acceptor. The result can be seen in Table 2.

The results above show that out of the 20 compounds found in the ethanol extract of Matoa leaves (*Pometia pinnata*), 17 met the criteria for Lipinski's Rule of Five. The compounds that did not meet the criteria include apigenin 7-O-diglucuronide, nicotiflorin, and quercetin-3-O-glucosyl-(1→4)-rhamnoside (rutin). These compounds failed to meet at least two of the rule's criteria, suggesting they are less likely to have good oral bioavailability as potential drugs (Roskoski Jr 2023). Lipinski's Rule of Five is a guideline to evaluate the potential oral bioavailability of drug-like molecules. If

Table 2. Physicochemical properties of ethanol extract of *Pometia pinnata* leaf compound.

Compound	Molecular Weight	LogP	HBD	HBA
Apigenin 7-O-diglucuronide	622	-2.09	9	17
Benzene	78	1.68	0	0
Epigallocatechin	306	1.25	6	7
Gallic acid	170	0.50	4	5
Jasmonic acid	210	2.41	1	3
Kaempferol	286	2.30	4	6
Kaempferol-3-O-glucoside (astragalin)	448	-0.43	7	11
Kaempferol-3-O-rhamnoside (afzelin)	432	0.59	6	10
Nicotiflorin	594	-1.58	9	15
p-Coumaroyl glycolic acid	222	0.42	3	5
Phenol	94	1.39	1	1
p-hydroxybenzaldehyde	122	1.20	1	2
Quercetin	302	2.01	5	7
Quercetin-3-O-glucoside (isoquercetin)	464	-0.73	8	12
Quercetin-3-O-rhamnoside (quercitrin)	448	0.29	7	11
Quercetin-3-O-glucosyl-(1→4)-rhamnoside (rutin)	610	-1.87	10	16
Syringic acid	198	1.10	2	5
Tannin	1152	-4.91	2	24
Vanillic acid	168	1.09	2	4
Vanillin	152	1.21	1	3

a molecule violates one or more of these criteria, it is considered to have low bioavailability. The criteria include (1) molecular weight < 500 Da; (2) log P (lipophilicity) < 5; (3) hydrogen bond donors < 5; and (4) hydrogen bond acceptors < 10. A molecular weight exceeding 500 Da may reduce a compound's ability to penetrate cell membranes, affecting its solubility within the body (Lipinski 2004). Compounds with a LogP > 5 are highly hydrophobic and are more likely to stick to membranes than distribute into aqueous environments like cells or the bloodstream (Barber and Rostron 2021). The number of hydrogen bond donors must be less than 5 and 10 for the acceptors, as too many hydrogen bond donors in a drug molecule reduce its ability to penetrate the lipid bilayer of cells (Ivanović 2020).

The pharmacokinetics prediction was done using pkCSM; the results can be seen in Table 3.

The absorption activity of a compound is predicted using parameters such as water solubility, human intestinal absorption (HIA), and p-glycoprotein substrate. Water solubility measures a compound's ability to dissolve in water. The solubility range of the compounds tested was between -3.74 and -0.76, indicating that these compounds do not dissolve well in water but are more soluble in lipids. The intestine is a crucial organ for absorbing orally administered drugs, and HIA is used to predict how well a compound is absorbed in the intestines. A compound is considered well-absorbed if it has an absorption rate of more than 30%. According to the test results, compounds such as apigenin-7-O-diglucuronide, nicotiflorin, rutin, and tannins showed poor potential as oral drug candidates. P-glycoprotein, a transporter that expels toxins from cells, is also an important factor in drug development. Of the tested compounds, 12 were identified as p-glycoprotein substrates, while 8 were not, which will play a crucial role in determining their suitability for different routes of drug administration (Pires et al. 2015; Myung et al. 2024).

In predicting distribution properties, the critical parameters used are the steady-state volume of distribution (VDss) and the blood-brain barrier penetration (logBBB).

Table 3. Pharmacokinetics prediction of ethanol extract of *Pometia pinnata* leaves.

Compound	HIA (%)	Water solubility (log ml/L)	P-glycoprotein substrate	VDss	Log BBB	CYP3A4 substrate & inhibitor	Total clearance
Apigenin 7-O-diglucuronide	0	-2.87	Yes	-0.09	-1.94	No	-0.11
Benzene	95.90	-1.81	No	0.18	0.40	No	0.25
Epigallocatechin	48.17	-2.90	Yes	0.59	-1.44	No	0.53
Gallic acid	40.15	-1.91	No	-0.27	-1.42	No	0.62
Jasmonic acid	94.55	-2.11	No	-0.65	0.008	No	0.45
Kaempferol	84.95	-2.98	Yes	-0.17	-1.36	No	0.52
Kaempferol-3-O-glucoside (astragalin)	42.26	-3.36	Yes	-0.38	-1.67	No	0.68
Kaempferol-3-O-rhamnoside (afzelin)	57.49	-3.74	Yes	-0.54	-1.49	No	0.65
Nicotiflorin	27.58	-2.96	Yes	-0.21	-2.02	No	0.25
p-Coumaroyl glycolic acid	45.28	-1.82	Yes	-1.28	-0.88	No	0.39
Phenol	93.58	-0.89	No	-0.03	-0.04	No	0.25
p-hydroxybenzaldehyde	85.87	-0.76	No	-0.06	-0.20	No	0.58
Quercetin	74.80	-2.86	Yes	0.16	-1.58	No	0.47
Quercetin-3-O-glucoside (isoquercetin)	35.16	-2.99	Yes	-0.08	-1.91	No	0.65
Quercetin-3-O-rhamnoside (quercitrin)	50.39	-3.10	Yes	-0.15	-1.72	No	0.62
Quercetin-3-O-glucosyl-(1→4)-rhamnoside (rutin)	20.47	-2.90	Yes	-0.10	-2.25	No	0.06
Syringic acid	75.31	-1.72	No	-0.45	-0.36	No	0.72
Tannin	29.98	-2.89	Yes	0.01	-3.90	No	-3.37
Vanillic acid	75.00	-1.58	No	-0.45	-0.31	No	0.70
Vanillin	86.60	-1.69	No	-0.07	-0.19	No	0.63

VDss reflects the total volume into which a compound is distributed when the drug concentration stabilizes in blood plasma. From the table, only epigallocatechin exhibits a VDss value greater than 0.45. The ability of a drug to cross the blood-brain barrier is crucial for developing treatments targeting the brain. All compounds, except benzene, showed poor brain distribution. The metabolic capability of a compound is assessed through the parameters of CYP3A4 substrates and inhibitors. CYP3A4 is a vital detoxifying enzyme in drug metabolism, predominantly found in the liver. The results indicated that none of the compounds are substrates or inhibitors of CYP3A4, suggesting that this enzyme does not metabolize them. For excretory activity, total clearance was used as the parameter. Total clearance combines hepatic clearance (metabolism in the liver and biliary clearance) and renal clearance (excretion via the kidneys), predicting how long a compound remains in the bloodstream. The results show total clearance values ranging from -3.37 to 0.70, indicating that compounds with higher clearance values are excreted more rapidly (Pires et al. 2015; Myung et al. 2024).

The toxicity properties of the compounds can be seen in Table 4.

The toxicity parameters evaluated in this prediction include LD50 (lethal dose 50), hepatotoxicity, carcinogenicity, immunotoxicity, mutagenicity, and cytotoxicity. LD50 represents the dose required to cause death in 50% of a test population. The LD50 values obtained ranged from 10000 mg/kg to 159 mg/kg, indicating the compounds' toxicity range. An LD50 value of 10000 mg/kg suggests low toxicity (classified as practically non-toxic), while a 159 mg/kg value indicates moderate toxicity. LD50 is a crucial parameter for assessing the acute toxicity of a compound (Drwal et al. 2014). Hepatotoxicity refers to a compound's potential to cause liver damage at predicted exposure levels; none of the compounds exhibited hepatotoxicity in this prediction. Out of the 20 compounds, 6 of them, which are gallic acid, kaempferol-3-O-rhamnoside (afzelin), p-coumaroyl glycolic acid, p-hydroxybenzaldehyde, quercetin, and quercetin-3-O-rhamnoside (quercitrin), tested positive for carcinogenicity, indicating potential cancer-causing properties. This is important for understanding carcinogenic activity mechanisms and modifying these compounds to reduce cancer risk. However, a positive result for carcinogenicity does not necessarily mean the compound is harmful in all cases, as the prediction models are primarily based on specific animal models that may not fully replicate human physiology (Madia et al. 2019). Immunotoxicity, which assesses a compound's potential to impair immune function, was observed in five compounds: Kaempferol-3-O-rhamnoside (afzelin), nicotiflorin, quercetin-3-O-glucoside (isoquercetin), quercetin-3-O-rhamnoside (quercitrin), and quercetin-3-O-glucosyl-(1→4)-rhamnoside (rutin).

In some cases, compounds showing immunotoxicity could be helpful in therapeutic applications, particularly in conditions requiring immune modulation. Thus, it is essential to consider the broader context, including the therapeutic window, dose, and mechanism of action (Baldrick 2020). Only quercetin was found to be mutagenic, indicating its potential to cause genetic mutations, a factor that raises concerns about genetic damage and cancer risk. Finally, none of the compounds exhibited cytotoxicity,

Table 4. Toxicity prediction of compounds in ethanol extract of *Pometia pinnata* leaves.

Compound	LD50 (mg/kg)	Hepatotoxicity	Carcinogenicity	Immunotoxicity	Mutagenicity	Cytotoxicity
Apigenin 7-O-diglucuronide	5000	Inactive	Inactive	Inactive	Inactive	Inactive
Benzene	10000	Inactive	Inactive	Inactive	Inactive	Inactive
Epigallocatechin	10000	Inactive	Inactive	Inactive	Inactive	Inactive
Gallic acid	2000	Inactive	Active	Inactive	Inactive	Inactive
Jasmonic acid	180	Inactive	Inactive	Inactive	Inactive	Inactive
Kaempferol	3919	Inactive	Inactive	Inactive	Inactive	Inactive
Kaempferol-3-O-glucoside (astragalin)	5000	Inactive	Inactive	Inactive	Inactive	Inactive
Kaempferol-3-O-rhamnoside (afzelin)	5000	Inactive	Active	Active	Inactive	Inactive
Nicotiflorin	5000	Inactive	Inactive	Active	Inactive	Inactive
p-Coumaroyl glycolic acid	2000	Inactive	Active	Inactive	Inactive	Inactive
Phenol	270	Inactive	Inactive	Inactive	Inactive	Inactive
p-hydroxybenzaldehyde	250	Inactive	Active	Inactive	Inactive	Inactive
Quercetin	159	Inactive	Active	Inactive	Active	Inactive
Quercetin-3-O-glucoside (isoquercetin)	5000	Inactive	Inactive	Active	Inactive	Inactive
Quercetin-3-O-rhamnoside (quercitrin)	5000	Inactive	Active	Active	Inactive	Inactive
Quercetin-3-O-glucosyl-(1→4)-rhamnoside (rutin)	5000	Inactive	Inactive	Active	Inactive	Inactive
Syringic acid	1700	Inactive	Inactive	Inactive	Inactive	Inactive
Tannin	2260	Inactive	Inactive	Inactive	Inactive	Inactive
Vanillic acid	2000	Inactive	Inactive	Inactive	Inactive	Inactive
Vanillin	1000	Inactive	Inactive	Inactive	Inactive	Inactive

meaning they did not induce cell death at the concentrations tested. Therefore, all compounds are subjected to the next step, molecular docking (Banerjee et al. 2024).

Molecular docking analysis

This step consists of molecular docking validation of the receptor to the native ligand and molecular docking between the compounds with the receptor using Autodock Vina and DOCK6.2; the results can be seen in Fig. 1, Tables 5, 6.

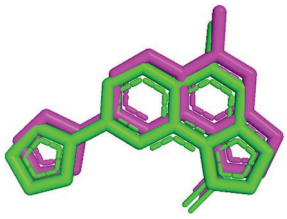

Figure 1. Docking validation of native ligand (green) and docked native ligand (pink).

The docking validation produced an RMSD of 0.990 Å, less than 2 Å, showing substantial similarity between the compared structures. This is evident from the similar positioning of the native and docked ligands (McNutt et al. 2021).

In Autodock Vina, the docking method used was rigid docking, where the ligand and the receptor were in the rigid position of the geometry, while in DOCK6.2, the docking process was performed in both rigid and flexible conditions, where the flexible docking allows both the ligand and receptor to move during the simulation, enabling a more accurate representation of molecular interactions in conditions that mimic the human body's dynamic environment. This approach provides a more precise and more detailed understanding of how the ligand and receptor behave under physiological conditions (Andrusier et al. 2008; de Ruyck et al. 2016).

The docking process using Autodock Vina produced binding affinities ranging from -4.6 to -9.3, with the native ligand, YEX, and Prexasertib (used as a reference drug) showing the lowest binding affinities. Binding affinity reflects the energy required for a compound and receptor to establish a stable interaction during the docking process; lower binding affinities indicate a stronger interaction, requiring less energy. In contrast, the DOCK6.2 results exhibited grid scores from -13.2196 to -66.4655, with compounds such as apigenin 7-O-diglucuronide, Kaempferol, Kaempferol-3-O-glucoside (astragalin), Kaempferol-3-O-rhamnoside (afzelin), Nicotiflorin, Quercetin, Quercetin-3-O-glucoside (isoquercetin), Quercetin-3-O-rhamnoside (quercitrin), Quercetin-3-O-glucosyl-(1→4)-rhamnoside (rutin), and Tannin having lower grid scores compared to

Table 5. Molecular docking results using Autodock Vina.

Compounds	H-Bond interaction	Hydrophobic bond interaction	Binding affinity
Apigenin 7-O-diglucuronide	GLU 17, ALA 19, LYS 132, ASN 135, SER 147	VAL 23, LYS 38, VAL 68, LEU 84, LEU 137	-8.3 ± 0.0
Benzene	-	LEU 15, VAL 23, ALA 36, CYS 87, LEU 137	-4.6 ± 0.0
Epigallocatechin	GLU 91	LEU 15, VAL 23, ALA 36, LEU 134, LEU 137	-8 ± 0.5196
Gallic acid	GLU 85, SER 147	LEU 15, VAL 23, ALA 36, LEU 137	-6 ± 0.0
Jasmonic acid	GLU 85	LEU 15, VAL 23, LEU 137	-6.767 ± 0.057
Kaempferol	GLU 85	VAL 23, ALA 36, VAL 68, LEU 84, LEU 137	-8.4 ± 0.0
Kaempferol-3-O-glucoside (astragalin)	GLY 16, GLU 17, SER 147, ASP 148	LEU 15, VAL 23, GLU 91, LEU 137	-7.267 ± 0.378
Kaempferol-3-O-rhamnoside (afzelin)	GLY 16, GLU 134, ASN 135, SER 147	GLU 91, LEU 137	-6.433 ± 0.057
Nicotiflorin	GLY 16, GLU 17, GLY 18, LYS 132, GLU 134, ASN 135, SER 147, ASP 148	LEU 15, VAL 23, LYS 132, GLU 134	-6.733 ± 0.057
p-Coumaroyl glycolic acid	GLU 17, GLU 85, CYS 87, GLU 134, ASN 135, SER 147	LEU 15, VAL 23, ALA 36, LEU 137	-7.1 ± 1.087
Phenol	-	LEU 15, VAL 23, ALA 36, LEU 137	-4.9 ± 0.0
p-hydroxybenzaldehyde	LEU 15, CYS 87, GLU 91	VAL 23, LEU 137	-5.5 ± 0.0
Quercetin	GLU 17	VAL 23, ALA 36, VAL 68, LEU 84, LEU 137	-8 ± 0.0
Quercetin-3-O-glucoside (isoquercetin)	GLY 16, GLU 134, ASN 135, SER 147, ASP 148	GLU 91, LEU 137	-6.6 ± 1.087
Quercetin-3-O-rhamnoside (quercitrin)	GLU 91, GLU 134, ASN 135	ALA 19, ASP 130, LYS 132	-6.2 ± 0.0
Quercetin-3-O-glucosyl-(1→4)-rhamnoside (rutin)	GLU 17, GLY 18, GLU 91, LYS 132, GLU 134, ASN 135, ASP 148	LEU 15, VAL 23, LYS 132, GLU 134	-6.7 ± 0.0
Syringic acid	GLU 17, GLU 85, SER 147	LEU 15, VAL 23, ALA 36, LYS 38, LEU 84, TYR 86, CYS 87, LEU 137	-6.3 ± 0.0
Tannin	GLU 91	LEU 15, VAL 23, ALA 36, LEU 137	-7.6 ± 0.1732
Vanillic acid	GLU 91	LEU 15, VAL 23, ALA 36, LEU 84, LEU 137	-6.2 ± 0.0
Vanillin	CYS 87, GLU 91	LEU 15, VAL 23, LEU 137	-6 ± 0.0
YEX (Native ligand)	GLY 18, GLU 55	LEU 15, VAL 23, ALA 36, VAL 68, LEU 84, LEU 137	-9.3 ± 0.0
Prexasertib	LEU 15, GLU 91, GLU 134, SER 147	ALA 36, LYS 38, LEU 84, LEU 137	-8.7 ± 0.0

Table 6. Molecular docking results using DOCK6.2.

Compounds	Rigid Docking		Flexible Docking		
	H-Bond interaction	Hydrophobic bond interaction	H-Bond interaction	Hydrophobic bond interaction	Grid Score
Apigenin 7-O-diglucuronide	LEU 15, GLY 16, LYS 38, CYS 87, ASP 94, ASP 148	LEU 15, VAL 23, LEU 137	TYR 86, CYS 87, SER 88, GLY 90, GLU 91, ASP 94, ASN 135	LEU 15, LEU 137	-55.9013 ± 0.0
Benzene	-	ALA 34		LEU 15, LEU 137	-13.2196 ± 0.0
Epigallocatechin	LEU 15, CYS 87, GLU 91, GLU 134	LEU 15, VAL 23, LEU 137	GLU 134, ASN 135	LEU 15, VAL 23, GLU 91, LEU 137	-41.7892 ± 0.0
Gallic acid	CYS 87, GLY 90, GLU 91	LEU 15, VAL 23, LEU 137	GLU 85	LEU 15, VAL 23, ALA 36, LEU 137	-27.5333 ± 0.0
Jasmonic acid	SER 147, ASP 148	-	GLY 16, GLU 17, GLU 134, SER 147	LEU 15, LEU 137	-35.0886 ± 0.0
Kaempferol	LYS 38, CYS 87, GLU 91, ASP 148	LEU 15, VAL 23, LEU 137	LYS 132, GLU 134, ASN 135, ASP 148	VAL 23, LEU 137	-48.1075 ± 0.0
Kaempferol-3-O-glucoside (astragalin)	GLU 17, GLU 91, ASN 135	GLU 91, LEU 137	LEU 15, CYS 87, SER 88, GLY 90, GLU 91	LEU 15, LEU 137	-57.9473 ± 0.0
Kaempferol-3-O-rhamnoside (afzelin)	GLN 13, TYR 86, CYS 87, GLY 90, GLU 91	LEU 15, GLU 91, LEU 137	GLU 17, LYS 132	GLU 91	-59.1781 ± 0.0
Nicotiflorin	THR 14, GLY 16, GLU 17, GLU 91	ASP 94	GLU 17, ASP 130, ASN 135, THR 170	GLU 91	-65.2588 ± 0.0
p-Coumaroyl glycolic acid	SER 147, ASP 148	LEU 15, LEU 137	CYS 87, SER 147, ASP 148	LEU 15, VAL 23, LEU 137	-36.2013 ± 0.0
Phenol	CYS 87	LEU 15, LEU 137	GLU 85	VAL 23, ALA 36, LEU 137	-17.1177 ± 0.0
p-hydroxybenzaldehyde	GLU 85, SER 147	VAL 23, ALA 36, LEU 137	CYS 87	LEU 15, LEU 137	-21.2022 ± 0.0
Quercetin	GLY 18, GLU 91, ASN 135	LEU 15, VAL 23	LYS 132, GLU 134, ASN 135, ASP 148	VAL 23, LEU 137	-49.5158 ± 0.0
Quercetin-3-O-glucoside (isoquercetin)	LEU 15, TYR 86, CYS 87, SER 88, GLY 90, GLU 91, ASP 94	LEU 15, LEU 137	GLU 17, GLU 91, ASN 135	GLU 91, LEU 137	-58.8390 ± 0.0
Quercetin-3-O-rhamnoside (quercitrin)	LEU 15, GLY 16, GLU 91, ASN 135, SER 147	GLU 17, LEU 137	GLU 91	GLU 91, LYS 132, ASN 135	-57.7804 ± 0.0
Quercetin-3-O-glucosyl-(1→4)-rhamnoside (rutin)	GLN 13, THR 14, TYR 86, GLY 90, GLU 91	LEU 15, ASP 94, LEU 137	GLU 17, ASP 130, ASN 135, THR 170	GLU 91	-66.4655 ± 0.0
Syringic acid	GLY 16, GLU 85, CYS 87	LEU 15, VAL 23, ALA 36, VAL 68, LEU 84, LEU 137	GLY 16, CYS 87, GLU 91	LEU 15, VAL 23, ALA 36, LEU 84, LEU 137	-31.6952 ± 0.0
Tannin	GLY 90, ASP 94, GLU 205	ASP 94, ARG 95, GLU 97, PHE 93, PRO 98	CYS 87, GLY 89, GLU 91, ASP 94, ASP 106	LEU 15, GLY 90, ASP 94, ARG 95	-65.4795 ± 0.0
Vanillic acid	GLY 18, SER 147, ASP 148	LEU 15, VAL 23, ALA 36, LEU 137	LEU 15, GLU 85, SER 147	VAL 23, ALA 36, LYS 38, LEU 84, LEU 137	-27.6175 ± 0.0
Vanillin	GLU 134, ASN 135, ASP 148	VAL 23, LEU 137	LYS 38, GLU 85	VAL 23, ALA 36, VAL 68, LEU 84, LEU 137	-25.6195 ± 0.0
YEX (Native ligand)	GLU 85, GLU 91	LEU 15, VAL 23, ALA 36, VAL 68, LEU 84, LEU 137	LEU 15, GLU 85, GLU 91	VAL 23, ALA 36, VAL 68, LEU 84, LEU 137	-44.34 ± 0.0
Prexasertib	LEU 15, GLU 85, SER 147	VAL 23, LEU 137	LEU 15, GLY 16, GLU 17, SER 147	VAL 23, ALA 36, CYS 87, GLU 91, LEU 137	-46.7221 ± 0.0

YEX and Prexasertib. Grid scores quantify binding energy, whereas lower scores correspond to more stable ligand-receptor interactions. The hydrogen bond interactions identified for the native ligand and Prexasertib in both Autodock Vina and DOCK6.2 involved critical amino acid residues, including LEU 15, GLU 85, GLU 91, GLU 134, and SER 147, suggesting these residues play a role in CHK1 inhibition. Research by Li et al. (2019) and Jin et al. (2021) supports the inhibitory activity of CHK1 through the formation of hydrogen bonds at additional residues, including GLY 16, GLU 17, GLY 18, GLU 55, CYS 87, ASN 135, and ASP 148. Hydrophobic interactions were also identified, with residues LEU 15, VAL 23, ALA 36, LYS 38, VAL 68, LEU 84, and LEU 137 contributing to the binding stability in both docking programs. Previous studies indicate hydrophobic interactions involving CYS 87 and GLU 91 further enhance CHK1 inhibition (Chen et al. 2010).

The docking analysis revealed that all compounds formed hydrogen bonds and hydrophobic interactions with key amino acid residues essential for CHK1 inhibition. Further evaluation identified five compounds with the best binding affinity and the most extensive hydrogen bonding, which were chosen for further validation through molecular dynamics simulations.

Molecular dynamic simulations

The simulations were run for 50 ns for each compound through GROMACS. The visualization throughout the 50 ns MD simulations can be seen in Fig. 2.

From the figure above, it can be seen that most of the ligands stay on the active site of the receptor throughout the 0 ns, 25 ns, and 50 ns trajectories except for Kaempferol-3-O-rhamnoside (afzelin) in 25 ns, which was out of the active site of the receptor. The ligand's ability to remain bound to the receptor's active site indicates stable binding interactions. This stability can be crucial for understanding the ligand's potential as a therapeutic agent, as it suggests that the ligand can maintain its activity over time, while a ligand that leaves the active site indicates unstable binding interactions. This instability suggests that the ligand may not maintain its activity over time, which could limit its therapeutic potential (Pieroni et al. 2023).

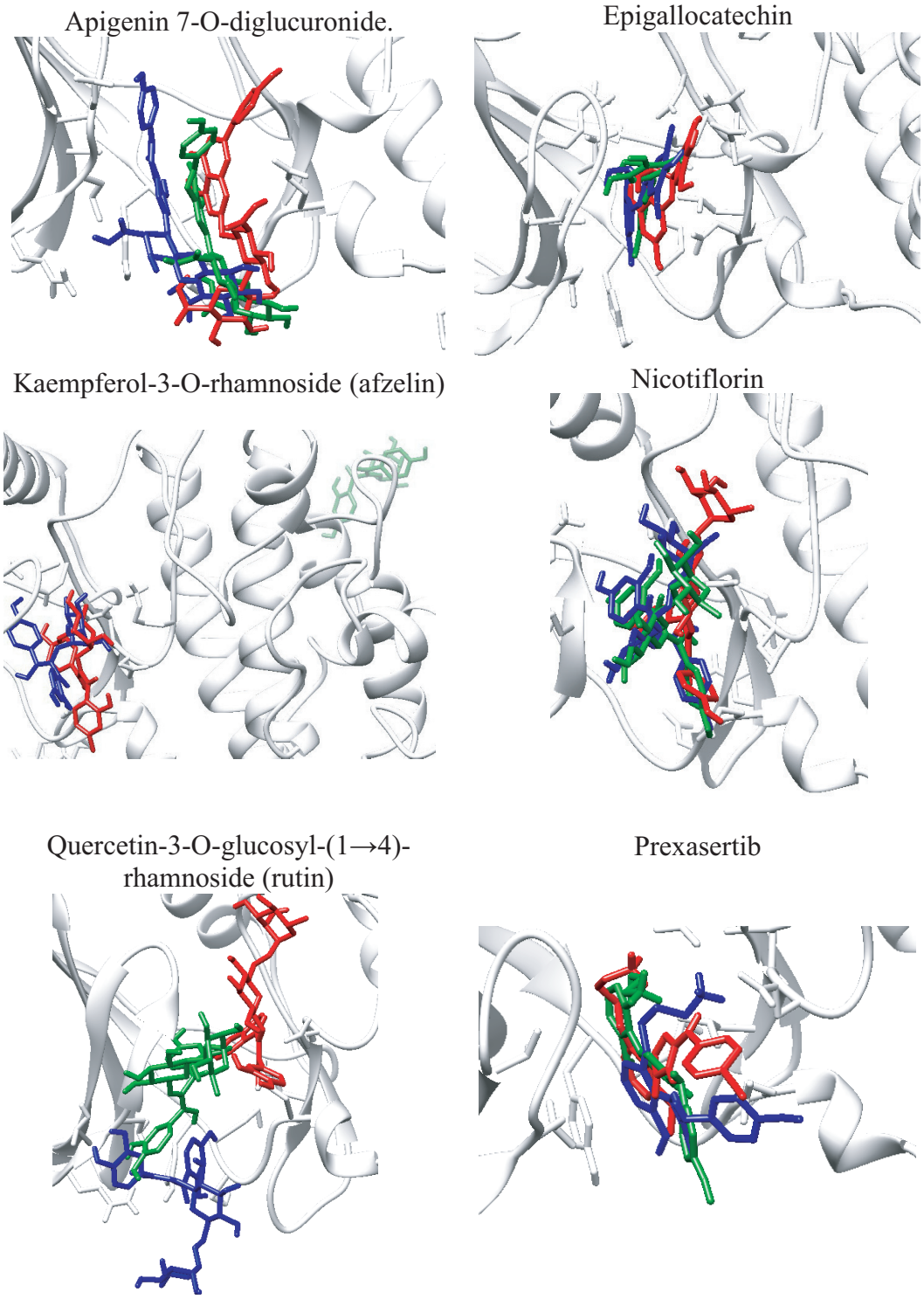

Figure 2. Visualization of ligands in 0, 25, and 50 ns.

Analysis of the RMSD, RMSF, SASA, and hydrogen bonds formed throughout the 50 ns simulation was captured and can be seen in Fig. 3.

RMSD (Root Mean Square Deviation) is commonly used to evaluate the stability and convergence of molecular dynamics simulations by measuring the average displace-

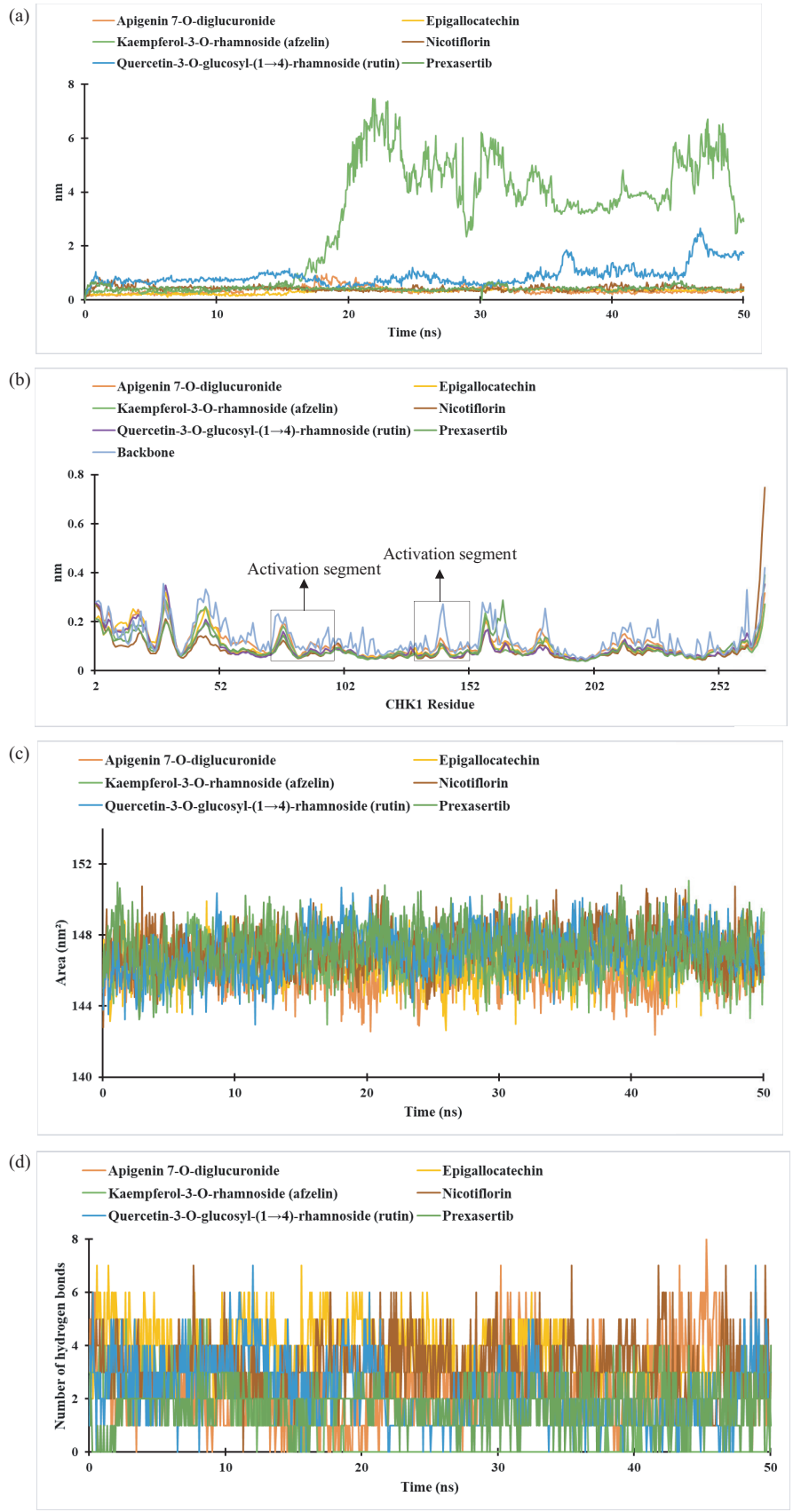

Figure 3. Results of: **a** RMSD; **b** RMSF; **c** SASA, and **d** hydrogen bonds of compounds to CHK1.

ment between atoms of superimposed structures over time. It provides insights into the extent of structural deviations from the initial configuration. In this study, the RMSD values of most compounds remained stable, except for kaempferol-3-O-rhamnoside (afzelin), which reached 6.8 nm after 15 ns, while other compounds ranged between 0.5 and 1.5 nm. Higher RMSD values suggest potential instability or conformational flexibility, which may impact the biological activity of the ligand or receptor. RMSF (Root Mean Square Fluctuation) measures the flexibility of individual residues or atoms within a molecular system during an MD simulation. It provides insights into which parts of a molecule are more dynamic and which are rigid. Low RMSF values indicate stable regions essential for maintaining structural integrity and function, while higher values suggest flexibility that could be important for ligand binding or protein activity.

The simulations showed RMSF values between 0.05 and 0.74 nm, suggesting that most atoms within the protein or ligand exhibit low fluctuation, indicating stability. The activation segment, critical for the protein's ability to phosphorylate substrates, was observed between residues 80–95 and 130–150, aligning with the CHK1 binding pocket interactions, particularly involving GLU 85, CYS 87, GLU 91, GLU 134, ASN 135, SER 147, and ASP 148. Activation in this segment results in CHK1 inhibition. Analysis of solvent accessible surface area (SASA) is important to understanding molecular interactions, such as ligand binding and protein folding. It provides insights into how much of a molecule is exposed to solvent, which can influence interactions and stability with other molecules. The simulations form a stable SASA interaction with values ranging from 143 to 151 nm^2, indicating that the protein or ligand's solvent-exposed surface remained stable throughout the simulation, maintaining ligand accessibility to the binding site. The number of hydrogen bonds provides insight into molecular stability and interaction strength between ligands and receptors. A higher number of hydrogen bonds typically correlates with increased complex stability. The hydrogen bonds formed ranged from 0 to 8, with apigenin 7-O-diglucuronide having the highest hydrogen bonds. The presence of hydrogen bonds is crucial for stabilizing protein structures and ligand-receptor interactions; thus, fluctuations in this range could imply dynamic interactions and increased stability of a complex (Zhao et al. 2015; Tanwar and Doss 2018; Hashemzadeh et al. 2020; Horx and Geyer 2020; Maruyama et al. 2023; Yekeen et al. 2023).

The amino acid residues formed in hydrogen and hydrophobic interaction were also analyzed along with the MMPBSA value; the results can be seen in Table 7.

The amino acid residues in hydrogen bond interaction were formed in GLU 17, CYS 87, and GLU 91, suggesting these residues play a role in CHK1 inhibition. Research by Jin et al. (2021) and Li et al. (2019) supports the inhibitory activity of CHK1 through the formation of hydrogen bonds at additional residues, including LEU 15, GLU 17, GLU 85, CYS 87, GLU 134, ASN 135, and ASP 148. The hydrophobic bond interaction was formed in amino acid residues LEU 15, VAL 23, VAL 36, TYR 86, GLU 91, LEU 137, and ASP 148, and all compounds formed the hydrophobic bonds in the identical amino acid residues.

As for the MMPBSA analysis, the value of $\boldsymbol{E}_{\mathbf{VDW}}$ (van der Waals energy), $\boldsymbol{E}_{\mathbf{ELE}}$ (electrostatic energy), $\boldsymbol{E}_{\mathbf{polar}}$ (polar solvation energy), $\boldsymbol{E}_{\mathbf{non\text{-}polar}}$ (nonpolar solvation energy), and $\boldsymbol{E}_{\mathbf{GTOTAL}}$ (total energy). The van der Waals energy represents the attractive and repulsive forces between non-bonded atoms, which significantly stabilize the ligand within the binding site. Electrostatic energy, on the other hand, accounts for the electrostatic interactions between charged groups, which are critical for the specificity and strength of binding. The polar solvation energy term quantifies the contribution of polar solvation, calculated using continuum models like the Poisson-Boltzmann equation, reflecting how solvent affects the stability of the protein-ligand complex. The nonpolar solvation energy term models the contribution from nonpolar solvation effects, often related to the ligand's solvent-accessible surface area (SASA), which accounts for the energetic cost of cavity formation in the solvent. Finally, the total energy is the sum of these energy components and represents the overall binding affinity of the ligand to its target (Genheden and Ryde 2015; Wang et al. 2018; Akkus et al. 2023). The MMPBSA values of the compounds are lower than those of the standard drug, Prexasertib. This suggests that all the compounds exhibit stable interactions with the target ligand. As a result, the ethanol extract of *Pometia pinnata* leaves warrants further investigation through in vitro cytotoxicity assays.

Cytotoxicity assay to cell MCF-7

The cytotoxicity assay was conducted using the MTT method on MCF-7 cells; this assay calculated the percentage of viable cells and the IC_{50} value, as seen in Graphic 1 and Table 8.

Table 7. Amino acid residues and MMPBSA of compounds to CHK1.

Compounds	Amino Acid Residue		MMPBSA				
	H-bond interaction	Hydrophobic bonds interaction	ΔE_{VDW}	ΔE_{ELE}	ΔE_{polar}	$\Delta E_{non\ polar}$	ΔE_{GTOTAL}
Apigenin 7-O-diglucuronide	THR 14, GLU 17, TYR 86, SER 88	LEU 15, VAL 23, ALA 36	-45.40	-51.22	77.02	-7.00	-26.60
Epigallocatechin	GLU 85, CYS 87, GLU 91, ASP 148	ALA 36, LEU 137	-32.40	-43.75	55.64	-5.12	-25.64
Kaempferol-3-O-rhamnoside (afzelin)	LEU 15, ALA 19, GLU 134, ASN 135, ASP 148	VAL 23	-24.37	-18.70	31.81	-4.16	-15.43
Nicotiflorin	GLU 17, GLU 91, GLU 134, ASP 148	-	-21.03	-30.50	43.30	-3.54	-11.77
Quercetin-3-O-glucosyl-(1→4)-rhamnoside (rutin)	THR 14, CYS 87, SER 88	LEU 15	-21.29	-47.35	60.78	-3.87	-11.74
Prexasertib	GLU 17, CYS 87, GLU 91	LEU 15, VAL 23, VAL 36, TYR 86, GLU 91, LEU 137, ASP 148	-28.32	-537.74	560.53	-5.37	-10.91

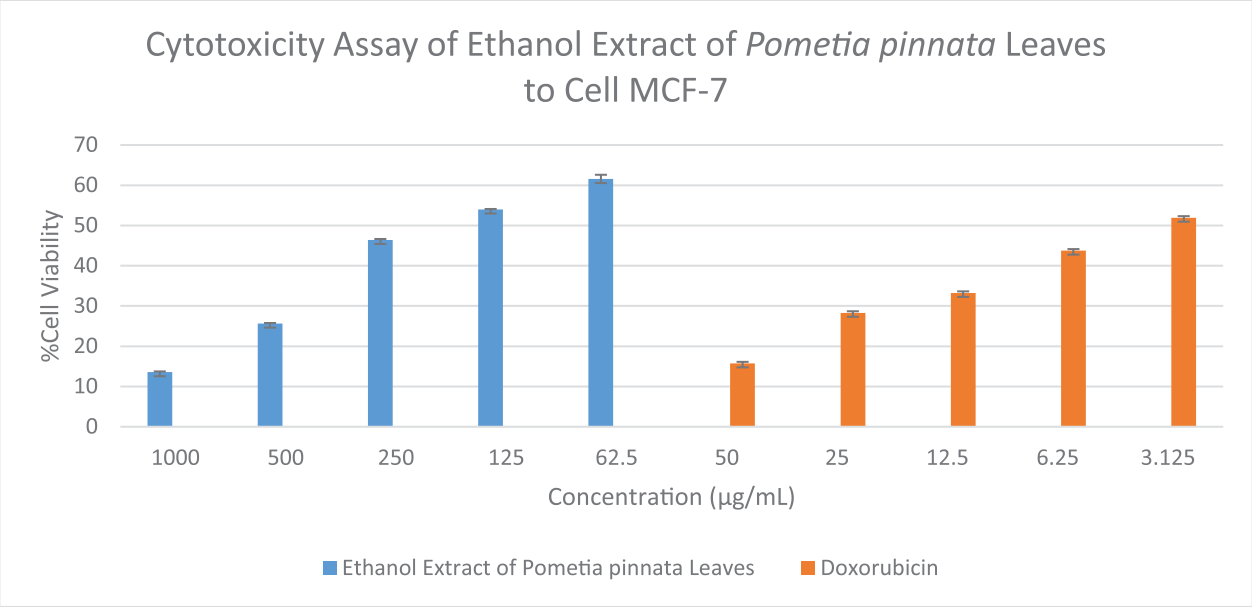

Graphic 1. Cell viability percentage of MCF-7 cells treated with ethanol extract of *Pometia pinnata* leaves and doxorubicin.

Table 8. IC_{50} value of ethanol extract of *Pometia pinnata* leaves and doxorubicin to cells MCF-7.

Value	Ethanol Extract of *Pometia pinnata* Leaves	Doxorubicin
IC_{50} (µg/mL)	139.38 ± 1.12	7.76 ± 1.06

In the cytotoxicity assay, the concentrations used for the ethanolic extract of *Pometia pinnata* were 1000, 500, 250, 125, and 62.5 µg/mL. These concentrations were selected based on commonly applied variations in studies involving plant ethanol extracts, where concentrations typically range from 10 to 1000 µg/mL. Furthermore, the previous research on the cytotoxic activity of *Pometia pinnata* extract utilized concentrations from 500 to 1500 µg/mL in a brine shrimp lethality test (BSLT). For doxorubicin, the concentrations used ranged from 50, 25, 12.5, 6.25, and 3.125 µg/mL. Doxorubicin is commonly used in concentrations of 0.25 to 150 µg/mL, which allows for the establishment of a dose-response curve and the determination of the IC_{50} value effectively. This range of concentrations enables a comprehensive assessment of the cytotoxic potential of the *Pometia pinnata* ethanol extract in cancer cells (Wang et al. 2014; Rahmawati et al. 2024).

The graphic above shows that the cell's viability decreases as the compound's concentration increases, showing that the ethanol extract of *Pometia pinnata* leaves can cause inhibitory activity in the cell. The method used in this experiment is the MTT assay, a standard method employed to assess the cytotoxic effects of compounds. The MTT assay measures the reduction of the yellow tetrazolium salt, 3-(4,5-dimethylthiazol-2-yl)-2,5-diphenyltetrazolium bromide (MTT), to purple formazan crystals by mitochondrial enzymes in viable cells. This reduction occurs primarily in metabolically active cells, indicating that the cells are alive and functioning normally. When cells are exposed to compounds, the metabolic activity diminishes as cell viability decreases. Consequently, fewer viable cells lead to a reduced amount of formazan produced, which can be quantitatively measured using a microplate reader at an absorbance wavelength of 570 nm. This method also allows for determining the IC_{50} value, representing the compound concentration required to inhibit cell growth by 50% (Ghasemi et al. 2021; Purwaningsih et al. 2021). The results from these assays help identify compounds that exhibit significant cytotoxicity against cells, thereby indicating their potential as anticancer agents. The cell used in this assay is MCF-7, a luminal breast cancer cell whose growth depends on estrogen receptors. This cell is commonly used in studies developing the potential anticancer compound to treat breast cancer, as it is a poorly aggressive and non-invasive cell and is considered to have low metastatic potential (Comsa et al. 2015). Doxorubicin is a positive control used in this experiment where it is known to be an FDA-approved chemotherapy agent; it works by intercalating into DNA, inhibiting topoisomerase II, disrupting mitochondria function, and potentiating oxidative damage to cancer cells (Kciuk et al. 2023).

Molyneux (2004) classified half-maximal inhibitory concentration activity based on IC_{50} values, with compounds exhibiting high cytotoxic activity if the IC_{50} value is < 50 µg/mL, vigorous activity between 50 and 100 µg/mL, moderate activity between 101 and 150 µg/mL, and weak activity if the IC_{50} value is > 150 µg/mL. According to this classification, the ethanol extract of *Pometia pinnata* leaves demonstrates moderate cytotoxic activity. At the same time, Doxorubicin shows very strong cytotoxic activity, consistent with the findings of Yusuf et al. (2020), who reported an IC_{50} value of 5.074 µg/mL for Doxorubicin. The moderate cytotoxic activity results of *Pometia pinnata* extract may indicate that its therapeutic effects are not fully optimized, but it still shows potential.

Further studies using assays such as proliferation inhibition and apoptosis induction could provide additional insights into its anticancer properties. Additionally, testing the extract on a broader range of cancer cell lines could reveal different levels of sensitivity and potentially uncover cancer types in which the compound is more effective.

Conclusion

The overexpression of CHK1 is commonly observed in many cancer types, establishing CHK1 as a critical pathway in cancer progression. Inhibiting CHK1 could reduce cancer incidence, making the development of CHK1 inhibitors essential in anticancer drug discovery. The extracts show the presence of flavonoids, alkaloids, tannins, saponins, glycosides, and steroids that contribute to the potential anticancer activity of the extract. Prediction of physicochemical, pharmacokinetic, and toxicity properties of compounds revealed that only some compounds met the required parameters; however, because of some limitations in their predicted profiles, these compounds will still advance to the next step of analysis, including molecular docking, to fully explore their potential interactions and efficacy. Molecular docking and molecular dynamics simulations of compounds from the ethanol extract of *Pometia pinnata* leaves revealed that 5 out of 20 compounds displayed strong, stable interactions with CHK1, as indicated by favorable binding affinity, grid scores, and MMPBSA scores. These interactions involve hydrogen and hydrophobic interactions with critical amino acid residues, further supported by in vitro cytotoxicity assays on MCF-7 cells. The ethanol extract demonstrated cytotoxic activity, as evidenced by decreased viable MCF-7 cells with increasing extract concentration. Additionally, the extract exhibited a moderate IC_{50} value against MCF-7 cells.

Acknowledgements

The authors are thankful to the Faculty of Pharmacy, Universitas Sumatera Utara, and the Faculty of Medicine, Public Health, and Nursing, Universitas Gadjah Mada, for the assistance, support, and for facilitating the study.

Additional information

Conflict of interest

The authors have declared that no competing interests exist.

Ethical statements

The authors declared that no clinical trials were performed for the present study.

The authors declared that no experiments on animals were performed for the present study.

The authors declared that experiments on humans or human tissues were performed for the present study with research ethics approval from Animal Research Ethics Committee of the Faculty of Mathematics and Natural Sciences – Universitas Sumatera Utara, with document number 0670/KEPH-FMIPA/2021.

Funding

The authors sincerely grateful for the financial support by the Ministry of Education, Culture, Research, and Technology through Penelitian Fundamental Reguler Kompetitif Nasional, under contract number 15/UN5/4.10.S/PPM/KP-DRTPM/2024.

Author contributions

H.S.W. conceptualizing, performed the experiment, analyzed the data, drafted the manuscript, revised and corrected the manuscript. M. performed the experiment, analyzed the data, revised and corrected the manuscript. S.E.N. performed the experiment, collected the data, revised and corrected the manuscript. I.B.S. performed the experiment, collected the data, revised and corrected the manuscript. C.C.J. performed the experiment. T.B.H. performed the experiment. All authors have read and agreed to the published version of the manuscript.

Author ORCIDs

Henny Sri Wahyuni https://orcid.org/0000-0002-7646-2928
Marianne https://orcid.org/0000-0003-4378-8611
Sony Eka Nugraha https://orcid.org/0000-0001-8849-2481
Imam Bagus Sumantri https://orcid.org/0000-0003-4462-167X
Clara Claudia Jap https://orcid.org/0009-0007-6363-8334

Data availability

All of the data are available in the main manuscript.

References

Akkus E, Tayfuroglu O, Yildiz M, Kocak A (2023) Revisiting MMPBSA by adoption of MC-based surface area/volume. ANI-ML Potentials, and Two-Valued Interior Dielectric Constant the Journal of Physical Chemistry B 127: 4415–4429. https://doi.org/10.1021/acs.jpcb.3c00834

Andrusier N, Mashiach R, Nussinov HJ, Wolfson HJ (2008) Principles of flexible protein-protein docking. Proteins 73(2): 271–289. https://doi.org/10.1002/prot.22170

Baldrick P (2020) Nonclinical immunotoxicity testing in the pharmaceutical world: The past, present, and future. Therapeutic Innovation & Regulatory Science 54(3): 586–597. https://doi.org/10.1007/s43441-019-00091-5

Banerjee P, Kemmler E, Dunkel M, Preissner R (2024) ProTox 3.0: A webserver for predicting toxicity of chemicals. Nucleic Acids Research 52(W1): 513–520. https://doi.org/10.1093/nar/gkae303

Bauer P, Hess B, Lindahi E (2022) GROMACS 2022.4 Manual. Zenodo 2022.

CCRC (2009) Protokol. https://ccrc.farmasi.ugm.ac.id/protokol/ [Accessed on 02.09.2024]

Chen XM, Lu T, Lu S, Li HF, Yuan HL, Ran T, Liu HC, Chen YD (2010) Structure-based and shape-complemented pharmacophore modeling for discovering novel checkpoint kinase 1 inhibitors. Journal of Molecular Modeling 16(7): 1195–1204. https://doi.org/10.1007/s00894-009-0630-y

Comsa S, Cimpean AM, Raica M (2015) The story of MCF-7 Breast cancer cell line: 40 years of experience in research. Anticancer Research 35: 3147–3154.

de Ruyck J, Brysbaert G, Blossey R, Lensink MF (2016) Molecular docking as a popular tool in drug design, an in silico travel. Advances and Applications in Bioinformatics and Chemistry 9: 1–11. https://doi.org/10.2147/AABC.S105289

Dhyani P, Quispe C, Sharma E, Bahukhandi A, Sati P, Attri DC, Szopa A, Sharifi-Rad J, Docea AO, Mardare I, Calina D, Cho WC (2022) Anticancer potential of alkaloids: A key emphasis to colchicine, vinblastine, vincristine, vindesine, vinorelbine and vincamine. Cancer Cell International 22(1): 206–226. https://doi.org/10.1186/s12935-022-02624-9

Drwal MN, Banerjee P, Dunkel M, Wettig MR, Preissner R (2014) ProTox: A web server for the in silico prediction of rodent oral toxicity. Nucleic Acids Research 42(W1): 53–58. https://doi.org/10.1093/nar/gku401

Duyen NT, Vinh LB, Phong NV, Khoi NM, Ha DT, Long PQ, Dung LV, Hien TT, Dat NT, Lee KY (2022) Steroid glycosides isolated from Paris polyphylla var. chinensis aerial parts and paris saponin II induces G1/S-phase MCF-7 cell cycle arrest. Carbohydrate Research 519: 108613–108619. https://doi.org/10.1016/j.carres.2022.108613

Edirweera MK, Tennekoon KH, Samarakoon SR (2018) In vitro assays and techniques utilized in anticancer drug discovery. Journal of Applied Toxicology 39(1): 38–71. https://doi.org/10.1002/jat.3658

GCO (2020) Cancer Today. https://gco.iarc.fr/today/ [Accessed on 14.08.2024]

Genheden S, Ryde U (2015) The MM/PBSA and MM/GBSA methods to estimate ligand-binding affinities. Expert Opinion on Drug Discovery 10(5): 449–461. https://doi.org/10.1517/17460441.2015.1032936

Ghasemi M, Turnbull T, Sebastian S, Kempson I (2021) The MTT assay: Utility, limitations, pitfalls, and interpretation in bulk and single-cell analysis. International Journal of Molecular Sciences 22(23): 12827–12857. https://doi.org/10.3390/ijms222312827

Hashemzadeh H, Javadi H, Darvishi MH (2020) Study of structural stability and formation mechanisms in DSPC and DPSM liposomes: A coarse-grained molecular dynamics simulation. Scientific Reports 10(1): 1837–1846. https://doi.org/10.1038/s41598-020-58730-z

Hollingsworth SA, Dror RO (2018) Molecular dynamics simulation for all. Neuron 99(6): 1129–1143. https://doi.org/10.1016/j.neuron.2018.08.011

Horx P, Geyer A (2020) define a hinge-type connection's mobility range using molecular dynamics and metadynamics. PLoS ONE 15: 1–6. https://doi.org/10.1371/journal.pone.0230962

Ivanovic V, Rancic M, Arsic B, Pavlovic A (2020) Lipinski's rule of five, famous extensions and exceptions. Chemia Naissensis 3(1): 171–177. https://doi.org/10.46793/ChemN3.1.171I

Jayalie VF, Kotambunan C, Apriantoni R, Manuain DA, Hawariy S, Prajogi GB, Permata TBM, Handoko, Munandar A, Sekarutami SM, Gondhowiardjo S (2023) Epidemiology of 10 cancer types in indonesia: a multicenter study. Journal of Indonesian Radiation Oncology Society 14: 22–29.

Jin T, Wang P, Long X, Jiang K, Song P, Wu W, Xu G, Zhou Y, Li J, Liu T (2021) Design, synthesis, and biological evaluation of orally bioavailable CHK1 inhibitors active against acute myeloid leukemia. ChemMedChem 16(9): 1477–1487. https://doi.org/10.1002/cmdc.202000882

Kciuk M, Gielecinska A, Mujwar S, Kolat D, Kaluzinska-Kolat Z, Celik I, Kontek R (2023) Doxorubicin—An agent with multiple mechanisms of anticancer activity. Cells 12(4): 659–689. https://doi.org/10.3390/cells12040659

Kitaeva KV, Rutland CS, Rizvanov AA, Solovyeva VV (2020) Cell culture based in vitro test systems for anticancer drug screening. Frontiers in Bioengineering and Biotechnology 8: 322–331. https://doi.org/10.3389/fbioe.2020.00322

Lee J, Cheng JM, Swails MS, Yeom PK, Eastman JA, Lemkul S, Wei S, Buckner J, Jeong JC, Qi Y, Jo S, Pande VS, Case DA, Brooks CL III, MacKerell Jr AD, Klauda JB, Im W (2016) CHARMM-GUI input generator for NAMD, GROMACS, AMBER, OpenMM, and CHARMM/OpenMM simulations using the CHARMM36 additive force field. Journal of Chemical Theory and Computation 12(1): 405–413. https://doi.org/10.1021/acs.jctc.5b00935

Li Y, Peng J, Zhou Y, Li P, Li Y, Liu X, Siddique AN, Zhang L, Zuo Z (2018) Pharmacophore modeling, molecular docking and molecular dynamics simulations toward identifying lead compounds for Chk1. Computational Biology and Chemistry 76: 53–60. https://doi.org/10.1016/j.compbiolchem.2018.06.001

Lipinski CA (2004) Lead-and drug-like compounds: The rule-of-five revolution. Drug Discovery Today: Technologies 1(4): 337–341. https://doi.org/10.1016/j.ddtec.2004.11.007

Madia F, Worth A, Whelan M, Corvi R (2019) Carcinogenicity assessment: Addressing the challenges of cancer and environmental chemicals. Environment International 128: 417–429. https://doi.org/10.1016/j.envint.2019.04.067

Manic G, Obrist F, Sistigu A, Vitale I (2015) Trial Watch – Targeting ATM-CHK2 and ATR-CHK1 pathways for anticancer therapy. Molecular & Cellular Oncology 2(4): 1–65. https://doi.org/10.1080/23723556.2015.1012976

Maruyama Y, Igarashi R, Ushiku Y, Mitsutake A (2023) Analysis of protein folding simulation with moving root mean square deviation. Journal of Chemical Information and Modeling 13(5): 1529–1541. https://doi.org/10.1021/acs.jcim.2c01444

McNutt AT, Francoeur P, Aggrawal R, Masuda T, Meli R, Ragoza M, Sunseri J, Koes DR (2021) GNINA 1.0: Molecular docking with deep learning. Journal of Cheminformatics 13(1): 1–20. https://doi.org/10.1186/s13321-021-00522-2

Molyneux P (2004) The use of the stable free radical diphenylpicrylhydrazyl (DPPH) for estimating antioxidant activity. Songklanakarin Journal of Science and Technology 26: 211–219.

Myung Y, de Sa AGC, Ascher DB (2024) Deepk-PK: Deep learning for small molecule pharmacokinetic and toxicity prediction. Nucleic Acids Research 52(W1): 469–475. https://doi.org/10.1093/nar/gkae254

Navien TN, Thevendran R, Hamdani HY, Tang TH, Citartan M (2021) In silico molecular docking in DNA aptamer development. Biochimie 180: 54–67. https://doi.org/10.1016/j.biochi.2020.10.005

Nikolaev A, Yang ES (2020) Combining CHK1/2 inhibition with radiation in head and neck cancer. In: Kimple RJ (Ed.) Improving the Therapeutic Ratio in Head and Neck Cancer. Elsevier, United States, 30–316. https://doi.org/10.1016/B978-0-12-817868-3.00014-7

Pieroni M, Madeddu F, Martino JD, Arcieri M, Parisi V, Bottoni P, Castrignano T (2023) MD–Ligand–Receptor: A high-performance computing tool for characterizing ligand–receptor binding interactions in molecular dynamics trajectories. International Journal of Molecular Sciences 24(14): 11671–11687. https://doi.org/10.3390/ijms241411671

Pires DEV, Blundell TL, Ascher DB (2015) pkCSM: Predicting small-molecule pharmacokinetic and toxicity properties using graph-based sig-

natures. Journal of Medicinal Chemistry 58(9): 4066–4072. https://doi.org/10.1021/acs.jmedchem.5b00104

Praptiwi, Wulansari D, Fathoni A, Harnoto N, Novita R, Alfridsyah, Agusta A (2020) Phytochemical screening, antibacterial and antioxidant assessment of *Leuconotis eugenifolia* leaf extract. Nusantara Bioscience 12(1): 79–85. https://doi.org/10.13057/nusbiosci/n120114

Purwaningsih E, Mustofa S Pendrianto (2021) Cytotoxicity Effects of Vitamin C on Cancer Cells MCF-7. In: Basic and Applied Science Conference (BASC) 2021 & First Education Research and Applied Business Conference, Malang (Indonesia), September 2021. Nusantara Science and Technology Proceedings, Malang-Indonesia, 15–20.

Rahmawati JE, Wati A, Handayani S (2024) Uji Aktivitas Sitotoksik Ekstrak Daun Matoa (*Pometia pinnata*) dengan Metode BSLT (Brine Shrimp Lethality Test). Makassar Pharmaceutical Science Journal 2: 99–112.

Rajasekar N, Sivananthan A, Ravikumar V, Rajasekaran S (2021) An overview on the role of plant-derived tannins for the treatment of lung cancer. Phytochemistry 188: 112799–112811. https://doi.org/10.1016/j.phytochem.2021.112799

Razoki (2023) Antioxidant and antibacterial activities of ethanol extract of Matoa (*Pometia pinnata*) leaves. Journal of Pharmaceutical and Sciences 6: 351–357.

Ronco C, Martin AR, Demange L, Benhida R (2016) ATM, ATR, CHK1, CHK2, and WEE1 inhibitors in cancer and cancer stem cells. MedChemComm 8(2): 295–319. https://doi.org/10.1039/C6MD00439C

Roskoski Jr R (2023) Rule of five violations among the FDA-approved small molecule protein kinase inhibitors. Pharmacological Research 191: 106774–106786. https://doi.org/10.1016/j.phrs.2023.106774

Rostron C, Barber J (2021) Pharmaceutical chemistry. 2nd edn. Oxford University Press, United Kingdom, 389 pp. https://doi.org/10.1093/hesc/9780198779780.001.0001

Roy A, Khan A, Ahmad I, Alghamdi S, Rajab BS, Babalghith AO, Alshahrani MY, Islam S, Islam MR (2022) Flavonoids a bioactive compound from medicinal plants and its therapeutic applications. BioMed Research International 2022: 1–9. https://doi.org/10.1155/2022/5445291

Shin D, Cho KH (2023) Critical transition and reversion of tumorigenesis. Nature 55: 692–705. https://doi.org/10.1038/s12276-023-00969-3

Suedee AT, Tewtrakul S, Panichayupakaranant P (2013) Anti-HIV-1 integrase compound from *Pometia pinnata* leaves. Pharmaceutical Biology 51(10): 1256–1261. https://doi.org/10.3109/13880209.2013.786098

Systemes D (2016) Biovia Discovery Studio. Dassault Syst mes, San Diego.

Tanwar H, Doss CGP (2018) An integrated computational framework to assess the mutational landscape of α-L-iduronidase IDUA gene. Journal of Cellular Biochemistry 119(1): 555–565. https://doi.org/10.1002/jcb.26214

Trott O, Olson AJ (2010) AutoDock Vina: Improving the speed and accuracy of docking with a new scoring function, efficient optimization and multithreading. Journal of Computational Chemistry 31(2): 455–461. https://doi.org/10.1002/jcc.21334

Wang X, Teng Z, Wang H, Wang C, Liu Y, Tang Y, Wu J, Sun J, Wang H, Wang J, Lu G (2014) Increasing the cytotoxicity of doxorubicin in breast cancer MCF-7 cells with multidrug resistance using a mesoporous silica nanoparticle drug delivery system. International Journal of Experimental Pathology 7: 1337–1347.

Wang C, Greene D, Xiao L, Qi R, Luo R (2018) Recent developments and applications of the MMPBSA method. Frontiers 4: 1–18. https://doi.org/10.3389/fmolb.2017.00087

Wiart C (2006) Medicinal plants of Asia and the Pacific. CRC Press, New York, 162 pp. https://doi.org/10.1201/9781420006803

Yekeen AA, Durojave OA, Idros MO, Muritala HF, Arise RO (2023) CHAPERONg: A tool for automated GROMACS-based molecular dynamics simulations and trajectory analyses. Computational and Structural Biotechnology Journal 21: 4849–4858. https://doi.org/10.1016/j.csbj.2023.09.024

Yusuf M (2023) Insights into the in-silico research: Current scenario, advantages, limits, and future perspectives. Life in Silico 1: 13–25.

Yusuf H, Satria D, Suryawati S, Fahriani M (2020) Combination therapy of eurycomanone and doxorubicin as anticancer on T47D and MCF-7 cell lines. Systematic Reviews in Pharmacy 11: 335–341.

Zhao Y, Zeng C, Massiah MA (2015) Molecular dynamics simulation reveals insights into the mechanism of unfolding by the A130T/V mutations within the MID1 Zinc-Binding Bbox1 Domain. PLoS ONE 10(4): 1–11. https://doi.org/10.1371/journal.pone.0124377